A modified potential for HO$_2$ with spectroscopic accuracy

João Brandão,[1,a)] Carolina M. A. Rio,[1] and Jonathan Tennyson[2]

[1]*Departamento Química Bioquímica e Farmácia, FCT, Universidade do Algarve, Campus de Gambelas, 8005-139 Faro, Portugal*

[2]*Department of Physics and Astronomy, University College London, Gower Street, London WC1E 6BT, United Kingdom*

Seven ground state potential energy surfaces for the hydroperoxyl radical are compared. The potentials were determined from either high-quality *ab initio* calculations, fits to spectroscopic data, or a combination of the two approaches. Vibration-rotation calculations are performed on each potential and the results compared with experiment. None of the available potentials is entirely satisfactory although the best spectroscopic results are obtained using the Morse oscillator rigid bender internal dynamics potential [Bunker *et al.*, J. Mol. Spectrosc. **155**, 44 (1992)]. We present modifications of the double many-body expansion IV potential of Pastrana *et al.* [J. Chem. Phys. **94**, 8093 (1990)]. These new potentials reproduce the observed vibrational levels and observed vibrational levels and rotational constants, respectively, while preserving the good global properties of the original potential. © *2009 American Institute of Physics.* [DOI: 10.1063/1.3103491]

I. INTRODUCTION

The hydroperoxyl radical HO$_2$ is an important intermediate in combustion as well as playing a role in interstellar chemistry. For this reason, and because HO$_2$ represents an intermediate in the reaction H+O$_2$↔O+OH, there have been many studies of the potential energy surface of its $\widetilde{X}\,^2A''$ ground state, see, for example, Refs. 1–10 and references included in those articles.

As a result of these studies there are a variety of potentials available for performing dynamical studies on HO$_2$, both in order to determine its rovibrational states and for modeling chemical reactions. Furthermore, in the commonly used many-body expansion (MBE) approach to building potential energy functions,[11] the potential of HO$_2$ represents an important, but relatively poorly defined, component of the potential of the important H$_2$O$_2$ molecule. For this reason we considered it worthwhile to undertake a systematic and critical survey of the potentials available for the HO$_2$ radical. Here we report the results of this study.

II. POTENTIAL ENERGY FUNCTIONS

Out of the published potentials which represent the potential minimum (minima) on the $\widetilde{X}\,^2A''$ ground electronic state of HO$_2$, we decided to test those potentials we consider to be the most accurate and those which cover the different procedures used in their construction. The seven potentials we choose[4–10] include the most accurate and recent ones. Below we consider them in turn, in order of date of publication.

The MBE potential of Farantos *et al.*[4] uses a MBE (Ref. 11) whose parameters have been fitted to reproduce the experimental geometry,[12] well depth,[13] and the harmonic force field deduced from the experimental vibrational data of Ogilvie.[12] The MBE potential does not include any correction for anharmonicity effects.

The DMBE IV potential of Pastrana *et al.*[5] is a double MBE potential.[14] It was mainly fitted to the *ab initio* points of Walch *et al.*,[15] semiempirically corrected using the DMBE-scaled-external correlation method,[16] augmented by *ab initio* data from the work of Melius and Blint,[17] and Walch and Rohlfing.[18] The potential was forced to reproduce the experimental equilibrium geometry,[19] dissociation energy,[15] and quadratic force constants[4,20] of the hydroperoxyl radical. Again the vibrational information was included using the harmonic force field.

The third potential is the Morse oscillator rigid bender internal dynamics (MORBID) function[21,22] due to Bunker *et al.*[6] This potential was obtained by fitting the more recent *ab initio* calculations of Walch and Duchovic,[23] and further points computed at the request of Bunker *et al.* Four parameters of the potential, so obtained, were adjusted using MORBID calculation to reproduce the four known vibrational energies[24,25] and associated rotational constants. The MORBID method is approximate which has been shown to give results with an average overestimate of the band origins by 1.1 cm^{-1} with a standard deviation of 6.4 cm^{-1} from those calculated using an exact kinetic energy operator for the H$_2$O molecule.[26] These errors are in turn reflected in potential functions fitted by this way. However, Bunker *et al.*[6] checked their MORBID results with an independent discrete variable representation (DVR) based method. It should be noted that our calculations reported below do not agree exactly with the DVR calculations of Bunker *et al.*,[6] being in close agreement (less than 0.5 cm^{-1}) with their MORBID results. The main discrepancies come from levels (100) and (200) where the differences are 1.1 and 4.7 cm^{-1}, respectively. Our implementation of the potential is precisely that given in the paper of Bunker *et al.* and, despite discussions with the authors, it

a)Electronic mail: jbrandao@ualg.pt.

remains unclear what is the cause of this discrepancy. Finally, the functional form used in this potential does not reproduce the symmetry needed to describe the exchange of the H atom between the two O atoms.

The Walch, Dateo, Duchovic (WDD) potential was constructed by Dateo[7] using the same *ab initio* data of Walch and Duchovic.[23] Although using a different functional form, the WDD surface has two- and three-body terms, each with short- and long-range terms, in a similar fashion to the DMBE method.

A different diatomics-in-molecules[27,28] (DIM) approach was taken by Kendrick and Pack.[8] Using the DIM model, Kendrick and Pack were able to fit accurately a large set of *ab initio* calculations from Walch and co-workers.[15,18,23,29,30] The DIM model is a multisurface approach and the DIM potential is able to correctly reproduce the conical intersections known to exist for HO_2 at C_{2v} and collinear geometries. All the other potentials used here are single valued surfaces which cannot reproduce these features. However, as pointed out by Kendrick and Pack, the diatomic potentials are based on Morse potentials and cannot accurately describe vibrationally excited states beyond the third vibrational level.

The next potential we use in this work is the DMBE IV-S potential of Varandas *et al.*[9] These authors adjusted the DMBE IV potential in order to reproduce the fundamental frequencies of the $H^{16}O_2$ radical.[25,31] This was achieved using rigorous vibrational calculations and a trial-and-error scaling of the internal coordinates. As noted by the authors, the scaling procedure they use slightly modifies the equilibrium properties of the original DMBE IV potential energy surface, and hence introduces small errors in the rotational constants relative to the unscaled surface.

Recently, Guo and co-workers[10,32,33] published a global analytical potential based on a cubic-spline fit of 15 000 high-quality (Davidson corrected internally contracted multireference configuration interaction or icMRCI+Q) *ab initio* points with a large (aug-cc-pVQZ) basis set, this new potential is denoted XXZLG PES. These authors comment that their potential energy surface (PES) provided a much improved agreement with experimental fundamental vibrational frequencies with errors less than 10 cm^{-1} as opposed to the 100 cm^{-1} found with the DMBE IV PES.[10] Lin *et al.*[34,35] also showed that the XXZLG PES gives much better agreement with the available spectroscopic data than the DMBE IV PES.

In summary, in this work we test potential energy surfaces with different genesis. They range from the exclusive use of the force field, MBE,[4] use of *ab initio* calculations and force field, DMBE IV,[5] mix of *ab initio* calculations and MORBID vibrational calculations,[6] only *ab initio* calculations fitted to a single valued function, WDD,[7] or to a DIM model, DIM,[8] using rigorous vibrational calculations, DMBE IV-S,[9] and the XXZLG PES (Ref. [10]) that is based on a cubic spline of about 15 000 *ab initio* points.

Of those potential energy surfaces, only the MORBID function of Bunker *et al.* does not aim to span all of configuration space. Designed for spectroscopic studies, this potential does not reproduce the dissociation to diatomic fragments nor the internal isomerization of HOO into OOH, a

TABLE I. Properties of the minimum and C_{2v} symmetry saddle point for the HO_2 electronic ground states potential energy surfaces used in this work.

	R_{O-O} (a_0)	R_{O-H} (a_0)	α_{OOH} (deg)	D_e [a] (E_h)
Minimum				
Empirical[b]	2.5144(16)	1.8344(38)	104.29(31)	−0.279 0
MBE[c]	2.570	1.861	106.0	−0.274 66
DMBE IV	2.5143	1.8345	104.29	−0.278 97
MORBID	2.5134	1.8358	104.31	⋯
WDD	2.5166	1.8357	103.84	−0.267 55
DIM	2.524	1.839	100.61	−0.274 07
DMBE IV-S	2.4930	1.8386	102.28	−0.278 97
XXZLG[d]	2.521	1.836	104.12	−0.273 69
DMBE IV-V	2.5143	1.8345	104.29	−0.278 97
DMBE IV-VR	2.5263	1.8588	106.08	−0.278 18

	R_{O-O} (a_0)	R_{O-H} (a_0)	α_{OHO} (deg)	V [e] (E_h)
Saddle point				
MBE[c]	2.422	2.205	66.63	0.066 8
DMBE IV	2.806	2.272	76.27	0.064 9
MORBID	⋯	⋯	⋯	⋯
WDD	2.686	2.184	75.89	0.061 1
DIM	2.663	2.207	74.21	0.060 4
DMBE IV-S	2.758	2.256	75.36	0.064 9
XXZLG[d]	2.724	2.192	76.80	0.061 3
DMBE IV-V	2.802	2.270	76.22	0.065 3
DMBE IV-VR	2.802	2.271	76.20	0.064 6

[a]Well depth energy relative to the three isolated atoms.
[b]See Refs. [15] and [19], values in parentheses represent estimated uncertainties.
[c]This potential has used, as input data, the experimental values given in Refs. [12] and [13].
[d]See Ref. [10].
[e]Relative to the bottom well.

process which is known to be allowed at all collision energies. All the other potentials are designed to reproduce the main features of the HO_2 potential energy surface.

Recent developments on the multiphoton technique capable of probing the vibration-rotation states of water just above and just below its dissociation limit with spectroscopic accuracy, see Ref. [36], and on the dynamics of the intramolecular energy transfer in the isotopic branching ratio on the O+HD reaction[37] have shown the necessity of global potential energy surfaces, accurate for all the configuration space and useful for both spectroscopic and dynamic studies. This is a goal nowadays feasible for small polyatomic systems.

A comparison of the predictions for the location, depth, and force field of the HO_2 potential minimum is given in Tables I and II. The last two rows of those tables refer to the new potentials (DMBE IV-V and DMBE IV-VR), proposed in this work, see Sec. IV for details. We note that only the MBE and DMBE IV potentials, although using different sources, were explicitly fitted in order to reproduce the experimental information available for the geometry, well depth, and force field. The MORBID, WDD, and DIM potentials used the *ab initio* energy values of Walch *et al.* as source data. The small differences we find in the predictions from those potentials came from the set of points used, the

TABLE II. Force constants for the HO$_2$ electronic ground state potential energy surfaces used in this work.

	F_{11} $(E_\mathrm{h}a_0^{-2})$	F_{22} $(E_\mathrm{h}a_0^{-2})$	$F_{\alpha\alpha}$ (E_h)	F_{12} $(E_\mathrm{h}a_0^{-2})$	$F_{1\alpha}$ $(E_\mathrm{h}a_0^{-1})$	$F_{2\alpha}$ $(E_\mathrm{h}a_0^{-1})$
Expt.[a]	0.3774	0.4286	0.2211	⋯	0.0414	⋯
MBE[b]	0.370	0.409	0.252	0.0093	0.0520	−0.0549
DMBE IV	0.377	0.429	0.221	0.0063	0.0414	−0.0621
MORBID	0.415	0.482	0.239	0.0161	0.0798	−0.0118
WDD	0.459	0.504	0.239	0.0142	0.0941	−0.0109
DIM	0.438	0.509	0.248	0.0189	0.0642	−0.0185
DMBE IV-S	0.401	0.455	0.258	−0.0156	0.0376	−0.0740
XXZLG	0.412	0.476	0.234	0.0140	0.0831	−0.0098
DMBE IV-V	0.420	0.468	0.271	−0.0426	0.0265	−0.0401
DMBE IV-VR	0.431	0.476	0.268	0.0104	0.0104	0.0168

[a]Fitted values neglecting the effect of the anharmonicity, see Ref. 20.
[b]This potential used a refinement by Mills and Carter of the force field given in Ref. 12.

functional form used, and from the quality of the fit. Note that the MORBID potential has been, in a second step, readjusted to reproduce observed spectroscopic data, and so, it has a slightly different harmonic force field. Comparing the properties of the DMBE IV and DMBE IV-S potentials, we can also see the effect of the scaling procedure used to adjust the DMBE IV-S potential.

It is interesting to note in Table II that the potentials fitted to the *ab initio* data or the observed vibrational frequencies have larger values for the force constants, in particular, F_{11}, F_{22}, and $F_{\alpha\alpha}$, when compared to the values deduced from experiment. This is particularly notable when comparing these values for the DMBE IV and DMBE IV-S potentials: the DMBE IV potential exactly reproduces the experimental force field, but the DMBE IV-S potential, which is a recalibration of the DMBE IV potential to reproduce the observed vibrational spectra, does not.

Another important feature, when computing spectra of this radical, is the saddle point for the exchange of the H atom between the two O atoms. In Table I we also compare the geometry and energy of this point on the different potentials. Bunker and co-workers pointed out that this feature (near 13 000 cm^{-1}) would not have a significant effect on the low-lying vibrational energies. Note, however, that its position determines the difference between odd and even states for the vibrational wave function. Our calculations below found differences between the amount of splitting between states which are odd and even with respect to the interchange of O atoms, see Barclay *et al.*,[38] for example, for the various potentials tested. For the highest states discussed below our calculation found splittings of about 0.001 cm^{-1} between odd and even symmetry calculations. Splittings of this magnitude are probably not significant, especially when one considers that this and previous studies ignore any effects of spin on the rotational levels. Furthermore, for H^{16}O$_2$ at least, this splitting cannot be determined experimentally, and for this reason we do not pursue this aspect of the problem here.

It has been pointed out that the $\widetilde{X}$ $^2A''$ ground state of the HO$_2$ radical correlates with a Π state at collinear geometries and, due to the degeneracy with the $\widetilde{A}$ $^2A'$ first excited state, the Renner–Teller effect should be considered.[39,40] However,

the collinear saddle point of the DMBE IV potential lies 17100 cm^{-1} above the bottom well, which is a high energy when compared to those used in our calculations. We have computed the probability of finding the system in configurations close to the collinear geometry,

$$\int_0^\alpha \left(\int_0^\infty \int_0^\infty \Psi^2(\theta,r,R)drdR \right) d\theta.$$

When using the wave function of (200) level for the DMBE IV potential, we find the probabilities to be 1.1×10^{-4}, 3.8×10^{-7}, and 1.3×10^{-10} for $\alpha=30°$, $\alpha=20°$, and $\alpha=10°$, respectively. We found lower values for the other levels. This results show that this probability fast decreases to zero as the system approaches collinearity and, similar to other calculations in the same systems,[9,35] the Renner–Teller effect can be neglected in this work.

Finally it should be noted that the low-lying excited electronic state, $\widetilde{A}$ $^2A'$, lies 7029 cm^{-1} above the ground state[24] and can thus be expected to perturb excited levels associated with the ground state. This should particularly be borne in mind when considering the highest observed vibrational band of the ground state, the (200) band, which is known experimentally to be perturbed.[24,41] Indeed in discussing their observations, Fink and Ramsay[42] appeared to doubt even the correctness of this assignment.

In their observational paper, Fink and Ramsay[42] concluded with a plea for better data on the vibrational levels of the ground potential energy surface at about 7000 cm^{-1} in order to identify the perturbed they identified in their spectra. We have analyzed the results of the calculations on each the potentials discussed above and find that none satisfy the criteria of Fink and Ramsay in terms of vibrational band origin and rotational constants.

The interaction between these two electronic states has been subject of accurate studies by Jensen and co-workers.[39,43,44] Using *ab initio* calculations on both states, these authors characterized the Renner–Teller effects at collinear geometries and the spin-orbit interaction between the $\widetilde{X}$(112) vibronic state and the $J\sim51/2$ rotational levels of the $\widetilde{A}$(000) state located at 7030 cm^{-1}. With reference to interaction between rovibrational states of the ground and

TABLE III. Experimental values for vibrational energies and for rotational constants (A, B, C), in cm^{-1}, the number in parentheses is one standard error in units of the last quoted digits.

	E_{vib}	A	B	C	Ref.
(000)		20.356 523 8(19)	1.118 034 0(17)	1.056 319 2(17)	59
(001)	1097.6258(1)	20.309 080 (50)	1.105 532(37)	1.042 649(38)	31
(010)	1391.7540(2)	20.957 46(67)	1.116 40(180)	1.050 08(183)	60
(100)	3436.1951(4)	19.584 15(67)	1.122 41(40)	1.058 25(37)	25
(200)	6651.1876(38)	18.903 3(17)	1.122 3(38)	1.050 8(21)	45

excited PESs, they comment that "at 7034 cm^{-1}, however, the $\widetilde{A}\ ^2A'$ rovibronic states emerge and interaction becomes more likely."[44] Furthermore, no such interaction between these two states has been observed in the 6603.2–6685.5 cm^{-1} region used to assign the $2\nu_1$ band constants[45] used in this work. As a consequence no off-diagonal electronic interactions are considered here when computing the rovibrational energies for the $\widetilde{X}(200)N=0$ or 1 states.

III. ROTATION-VIBRATION CALCULATIONS

Calculations were performed using the DVR3D program suite[46] in atom-diatom scattering coordinates which represent the O$_2$ as a diatomic with H as the atom. These coordinates are natural for the HO$_2$ molecule, but it should be noted that they automatically treat both symmetry-related minima in a nuclear motion calculation. This is a point discussed further below.

In our final calculations, the angular motions were represented using 40 grid points based on (associated) Legendre polynomials. Grids for both the O$_2$ stretch and H–O$_2$ stretch were based on the zeros of Morse oscillatorlike functions[46] which are associated Laguerre polynomials. These functions were characterized by parameter sets (r_e, D_e, w_e) (Ref. 46) equal, in atomic units, to (2.514,0.272 93,0.005 1204) and (2.467,0.102 89,0.013 2207), respectively. The final calculation used a grid of 28 points for the O$_2$ stretch and 20 points for the H–O$_2$ stretch. For $N=0$ calculations, a final Hamiltonian of dimension 3100 was diagonalized. For $N=1$ it was found that, in the second step of the calculation, a Hamil-

tonian of dimension 1000 was required to give converged results for the C rotational constant of the (200) state.

Extensive tests were performed to check the convergence of our rotation-vibration calculations. In particular, it was found necessary to perform quite large calculations for some potentials to obtain reliable results for the (200) vibrational state. This state varied between numbers 28 and 31 in our $J=0$ even calculations depending on which potential energy surface was used. In some cases the state shows heavy mixing with other vibrational modes. For each potential we assigned the (200) state on the basis of energy differences and expectation values for the radial O–O and H–OO distances. The OH stretching overtone should have a large $\langle R_{\text{H–OO}}\rangle$ value as well as a small value for $\langle R_{\text{O–O}}\rangle$. For the MBE, WDD, and DIM potentials, this method was unambiguous and allows us to assign it to the 31 (MBE) or 28 (WDD, DIM and XXZLG) levels. For the DMBE IV and DMBE IV-S potentials, we have been able to assign the level 31 to this state but, like Varandas et al.,[9] we found some mixing with level 30 that can be assigned to state (103). The coupling between two states, levels 29 and 30, is most evident for the MORBID potential which showed a particularly heavy mixing. As Bunker et al. fitted their potential to level 29, we chose to quote our results for this level. However, it should be noted that experimentally the assignment relies more heavily on transition intensity considerations which we have not tested in this work. Our final calculations are converged to within 0.1 cm^{-1} for the (200) state and much better than this for the lower vibrational term values. Within these error bars, our results agree with other accurate published results for these potentials.

TABLE IV. Calculated vibrational term values, in cm^{-1}, for the potentials used in this work.

	(001)	(010)	(100)	(200)	σ_{vib} [a]
Expt.[b]	1097.63	1391.75	3436.20	6651.19	
MBE	1075.54	1136.96	2871.77	5385.09	704.80
DMBE IV	1065.50	1296.40	3333.73	6492.37	107.06
MORBID	1097.47	1391.75	3436.49	6646.24[c]	2.48
WDD	1139.49	1413.75	3516.53	6783.33	80.86
DIM	1149.29	1410.30	3524.02	6794.63	88.46
DMBE IV-S	1097.83	1392.03	3436.59	6687.62	18.22
XXZLG	1089.97	1388.77	3433.09	6633.97	9.67
DMBE IV-V	1097.63	1391.75	3436.20	6651.19	0.00
DMBE IV-VR	1097.63	1391.75	3436.20	6651.19	0.00

[a]$\sigma_{\text{vib}}=\sqrt{(1/N)\Sigma_{i=1}^{4}(x_i^{\text{exp}}-x_i^{\text{cal}})^2}$, where x_i are the vibrational energies.
[b]See all figures and errors on Table III. For more detail see Refs. 25, 31, 45, and 60.
[c]Fitted to 6646.59 experimental data, Ref. 24.

TABLE V. Comparison, for the DIM potential (Ref. 8), between rotational constants, given in cm^{-1}, computed using expectation values or from energy levels, see Ref. 61.

State	From expectation values			From energy levels		
	A	B	C	A	B	C
(000)	19.75	1.113	1.053	19.74	1.117	1.053
(001)	19.71	1.099	1.039	19.70	1.103	1.039
(010)	20.37	1.107	1.048	20.36	1.117	1.049
(100)	19.02	1.115	1.049	19.02	1.119	1.053
(200)	18.32	1.115	1.045	18.31	1.122	1.052

The role of nuclear spin statistics in the levels of H^{16}O$_2$ has been the subject of some debate.[47] However, only states represented by even angular grid are spectroscopically observable and we only present results for these. This is in contrast to some other studies,[48–52] which have instead presented results only for the odd states.

Next, we compare our results with the experimental data quoted in Table III along with their quoted uncertainties.

Table IV compares the various vibrational term values computed in this work with the available experimental data. The MBE potential performs particularly poorly for the (100) H$-$O$_2$ stretching fundamental. The *ab initio* WDD potential is also 90 cm^{-1} in error for this mode and 50 cm^{-1} too high for the (001) bending fundamental. Perhaps not surprisedly, the two potentials which give the best estimates for the fundamentals are those which used these data directly in fitting: the MORBID and DMBE IV-S potentials. Comparing with these potentials, the *ab initio* XXZLG potential agrees better with experiment than the DMBE IV-S potential only for the (200) H$-$O$_2$ stretching overtone. Conversely the potentials which used harmonic data do not give a satisfactory representation of vibrational fundamentals.

Following Bunker *et al.*[6] and others, we assess the rotational data against experimentally determined rotational constants. From our DVR3D based procedure we used two ways of determining these constants. The first is by performing $N=1$ calculations and using the three rotational term values so determined to define the constants. This method assumes that centrifugal distortion effects are negligible for $N=1$ and that none of the $N=1$ levels in question are perturbed. For each state we calculate the three rotational energies for N $=1$ ($k=-1,0,1$), then we obtain the rotational constants (A, B, and C) using the following equations:

$$A = 0.5 \times (E_{10} + E_{11} - E_{1-1}),$$

$$B = E_{11} - A,$$

$$C = E_{10} - A. \tag{1}$$

The second method is to explicitly use the $N=0$ wave functions to give vibrational averages for the appropriate instantaneous, inverse inertia tensor using the program XPECT3 of the DVR3D suite.[46] We have compared these two approaches for all the potentials considered, and Table V summarizes the results obtained for the DIM potential which can be regarded as typical. The level of agreement between the two approaches is generally very good, even for the rotational constants of (200). Below we consider only results obtained using expectation values as the constants computed from our $N=1$ calculations proved rather sensitive to convergence of this calculation.

Table VI compares rotational constants obtained by us for all five vibrational states for which the corresponding constants have been experimentally determined. The DMBE IV and WDD potentials perform notably well for these constants, in contrast to their ability to reproduce the vibrational data. This is undoubtedly due to the accuracy with which these potentials reproduce the observed equilibrium structure (see Table I). Of the empirically determined potentials, only the MORBID potential, which is based about the correct equilibrium geometry, gives satisfactory rotational constants. Similar results have been found for the XXZLG *ab initio*
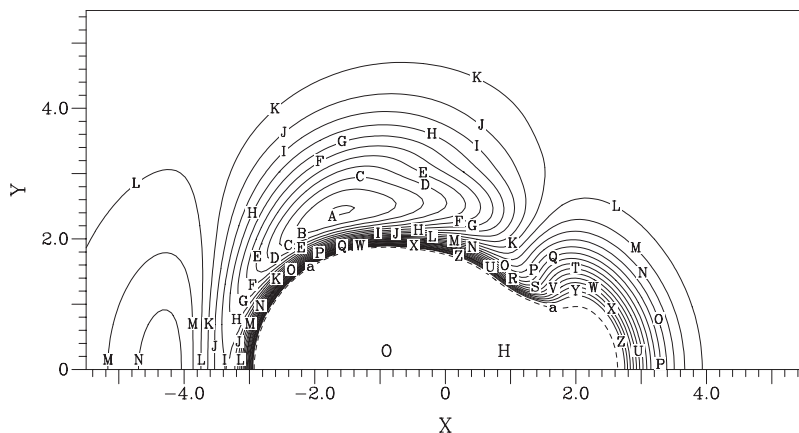

FIG. 1. Contour plot for the DMBE IV-VR potential for an O atom moving around an equilibrium OH diatomic with the center of the bond fixed at the origin. Contours are equally spaced by 0.01 E_h, starting at -0.277 E_h.

TABLE VI. Rotational constants, in cm^{-1}, calculated for the potentials used in this work.

		(000)	(001)	(010)	(100)	(200)	σ_{rot} [a]
	A	20.357	20.309	20.957	19.584	18.903	
Expt.[b]	B	1.118	1.106	1.116	1.122	1.122	
	C	1.056	1.043	1.050	1.058	1.051	
	A	20.43	20.43	21.92	29.04	485.89	
MBE	B	1.062	1.051	1.048	1.036	1.006	120.60
	C	1.008	0.997	0.997	0.990	0.974	
	A	20.46	20.21	21.25	19.68	18.95	
DMBE IV	B	1.118	1.094	1.119	1.125	1.117	0.089
	C	1.058	1.036	1.062	1.061	1.049	
	A	20.55	20.50	21.16	19.81	19.48	
MORBID	B	1.115	1.101	1.108	1.120	1.089	0.183
	C	1.056	1.043	1.050	1.056	1.026	
	A	20.50	20.46	21.18	19.76	19.36	
WDD	B	1.113	1.098	1.105	1.118	1.105	0.149
	C	1.054	1.040	1.047	1.055	1.040	
	A	19.75	19.71	20.37	19.02	18.32	
DIM	B	1.113	1.099	1.107	1.115	1.115	0.340
	C	1.053	1.039	1.048	1.049	1.045	
	A	19.89	19.70	20.57	19.06	18.69	
DMBE IV-S	B	1.143	1.119	1.142	1.151	1.130	0.266
	C	1.079	1.057	1.081	1.082	1.060	
	A	20.526	20.489	21.146	19.785	19.429	
XXZLG	B	1.109	1.095	1.101	1.113	1.087	0.167
	C	1.050	1.038	1.044	1.050	1.025	
	A	20.47	20.31	21.17	19.61	18.87	
DMBE IV-V	B	1.118	1.101	1.115	1.123	1.109	0.063
	C	1.058	1.043	1.057	1.059	1.042	
	A	20.36	20.31	20.95	19.58	18.90	
DMBE IV-VR	B	1.114	1.106	1.118	1.126	1.118	0.0024
	C	1.053	1.043	1.050	1.060	1.055	

[a]$\sigma_{rot} = \sqrt{(1/N)\Sigma_{i=1}^{15}(x_i^{exp} - x_i^{cal})^2}$, where x_i are the rotational constants.
[b]See all figures and errors on Table III. For more detail see Refs. 24, 25, 31, 45, 59, 60, and 62.

potential which also presents an equilibrium geometry close to experiment.

Most notably, the DMBE IV-S behaves poorly for the rotational constants. This potential, which gave excellent results for the vibrational fundamentals, is a scaled version of the DMBE IV potential which gives good results for the rotational constants. However, the method of scaling used is to adjust the geometric parameters to improve the estimates of the vibrational levels.[9] Such a procedure has been employed by Bowman and Gazdy[53,54] for other triatomic molecules.

The importance of the true potential of a molecule giving a reliable representation of both the vibrational *and* rotational levels of the molecule has been discussed at length elsewhere.[55] It would appear that the internal coordinate scaling procedure applied to the DMBE IV-S potential is bound by construction not to achieve this result. This raises serious concerns about what such potentials represent and hence the method used for their construction.

IV. MODIFIED DMBE IV-V AND VR POTENTIALS

Due to the high quality of the dynamical results obtained using the DMBE IV potential, we improve its spectroscopic properties by adding a small term to modify the bottom well,

while retaining the overall behavior of the PES in those regions that should play an important role in controlling the reaction dynamics in this system. The functional form used for this extra term is a polynomial multiplied by a quadratic exponential term in the displacement coordinates from the equilibrium geometry. To ensure the permutation symmetry of this system, we follow Schmelzer and Murrell[56] and define coordinates invariant to the exchange of the two oxygen atoms, i.e., the exchange of the R_2 and R_3 interatomic distances. Hence, the integrity basis is R_1, $S_1 = R_2 + R_3$ and $S_2 = (R_2 - R_3)^2$. Due to the existence of two symmetric minima in this system, we use as displacement coordinates,

$$R_{1d} = R_1 - R_{1eq},$$

$$S_{1d} = \frac{1}{\sqrt{2}}[(R_2 + R_3) - (R_{2eq} + R_{3eq})], \quad (2)$$

$$S_{2d} = \frac{1}{2}[(R_2 - R_3)^2 - (R_{2eq} - R_{3eq})^2],$$

where the values for R_{1eq}, R_{2eq}, and R_{3eq} are the quoted experimental equilibrium geometry[1] $2.5143a_0$, $1.8346a_0$, and $3.4592a_0$, respectively. These coordinates are simpler than those used in the DMBE IV PES and are all zero at the two equivalent reference geometries.

The functional form adopted for this additional term is a third degree polynomial (13 freely adjustable coefficients c_i) multiplied by a decay term with four fixed terms $c_{i\,fix}(i=1,2,3,4)$,

$$T = c_1 + c_2 R_{1d} + c_3 S_{1d} + c_4 R_{1d}^2 + c_5 S_{1d}^2 + c_6 R_{1d} S_{1d} + c_7 S_{2d}$$
$$+ c_8 R_{1d}^3 + c_9 R_{1d} S_{1d}^2 + c_{10} R_{1d}^2 S_{1d} + c_{11} R_{1d} S_{2d} + c_{12} S_{1d}^3$$
$$+ c_{13} S_{1d} S_{2d},$$

$$DEC = c_{1fix} R_{1d}^2 + c_{2fix} S_{1d}^2 + c_{3fix} R_{1d} S_{1d} + c_{4fix} S_{2d}^2, \qquad (3)$$

$$VR_{spect} = T \exp(- DEC).$$

To achieve the accuracy of 0.01 cm^{-1} necessary to fit the (200) state rotational constants, we changed to 80 grid points for the angular motions, 60 grid points for the O$_2$ stretch, and 40 grid points for the H$-$O$_2$ stretch, instead of the above referred 40, 28, 20 grid points used in the DVR3D integration.

The derivatives of the vibrational energies with respect to the coefficients were computed using the Hellmann–Feynman theorem,[57]

$$\frac{\partial E_n}{\partial c_i} = \int \Psi_n^* \frac{\partial \hat{H}}{\partial c_i} \Psi_n d\tau = \int \Psi_n^* \frac{\partial VR_{spect}}{\partial c_i} \Psi_n d\tau. \qquad (4)$$

The necessary integrals were evaluated using the package XPECT3 of the DVR3D suite[46] and the computed wave functions. The nonlinear fitting procedure was accomplished using the Marquardt algorithm.[58]

In a first step, we started fitting the four vibrational energies using only quadratic terms in Eq. (3), but with $c_7 S_{2d}^2$ to guarantee values of zero for the first derivatives at the equilibrium geometry, and in this way keep the same geometry, i.e.,

$$T = c_4 R_{1d}^2 + c_5 S_{1d}^2 + c_6 R_{1d} S_{1d} + c_7 S_{2d}^2. \qquad (5)$$

In this step we found that a constant value of 2.0 for the four fixed terms $c_{i\,fix}(i=1,2,3,4)$ in DEC was sufficient to yield an exact fit to the vibrational levels with minor changes in the rotational constants of the DMBE IV PES and confine this term to the region of the bottom well. We call this potential DMBE IV-V (and the reduced additional term, V_{spect}), where V stands for vibration only. As shown in Table VI this potential slightly improves the rotational constants.

In a second step, starting from this potential, we add three linear and six cubic terms to fit the rotational constants. Derivatives of the rotational constants were computed using the derivatives of the three rotational term values given by Eq. (1). To combine the vibrational and rotational constants in a same fit, we weigh the vibrational levels by 1.0, the A rotational constants by 10.0, and the B and C rotational constants by 100.0. The final potential, DMBE IV-VR, from vibration and rotation, still reproduces the vibrational energies with errors less than 0.005 cm^{-1} (see Table IV) and closely approaches the rotational constants with errors less than 0.0022, 0.0038, and 0.0042 cm^{-1}, for A, B, and C, re-

TABLE VII. Fitted coefficients, in a.u., for the DMBE IV-V and VR potentials.

	V_{spect}	VR_{spect}
c_1	$\cdots$	$1.094\ 421\ 9 \times 10^{-3}$
c_2	$\cdots$	$2.938\ 960\ 3 \times 10^{-4}$
c_3	$\cdots$	$-9.472\ 370\ 5 \times 10^{-3}$
c_4	$4.237\ 461\ 6 \times 10^{-2}$	$7.145\ 913\ 3 \times 10^{-2}$
c_5	$1.286\ 578\ 6 \times 10^{-2}$	$2.298\ 432\ 1 \times 10^{-2}$
c_6	$-5.257\ 641\ 3 \times 10^{-2}$	$-4.832\ 550\ 4 \times 10^{-2}$
c_7	$3.237\ 781\ 8 \times 10^{-3a}$	$4.723\ 445\ 0 \times 10^{-4}$
c_8	$\cdots$	$-5.977\ 740\ 9 \times 10^{-2}$
c_9	$\cdots$	$1.812\ 823\ 9 \times 10^{-2}$
c_{10}	$\cdots$	$6.418\ 464\ 3 \times 10^{-2}$
c_{11}	$\cdots$	$-1.138\ 416\ 1 \times 10^{-2}$
c_{12}	$\cdots$	$1.261\ 962\ 8 \times 10^{-3}$
c_{13}	$\cdots$	$-2.902\ 956\ 3 \times 10^{-3}$

[a]The coefficient c_7 is multiplied by S_{2d}^2, in the function T, see Eq. (3).

spectively (see Table VI). The fitted coefficients (c_i) obtained on the modified DMBE IV potentials are summarized on Table VII.

V. GENERAL OVERVIEW OF THE DMBE IV-V AND VR POTENTIALS

The general properties of these new DMBE IV-V and VR potentials are quoted in Tables I and II to compare with the other studied potentials. Comparing with the original DMBE IV potential, there we can see that both PESs display similar geometry for the C_{2v} saddle point, but while the DMBE IV-V potential has the same minimum geometry and energy, the DMBE IV-VR potential shows small changes on its position and energy. This result contrasts with previous findings linking the minimum position with the rotational constants, see comment on the DMBE IV-S potential in Sec. III and Table I.

Figure 1 shows a contour plot of the DMBE IV-VR PES for an O atom moving around an equilibrium OH molecule. This picture is similar to that of the original DMBE IV potential.[5] A perspective view for the VR_{spect} term is presented in Fig. 2 for the same geometries.

Another interesting view of those surfaces is shown in Figs. 3 and 4 where we plot the H atom moving around an equilibrium O$_2$ molecule. Figure 3 displays a contour plot for the additional term VR_{spect} and a close view of this term near the minimum geometry. There we can see that the main contribution is on the stretching of the OH bonding. In Fig. 4(a) we present the DMBE IV-VR and a close view of the bottom
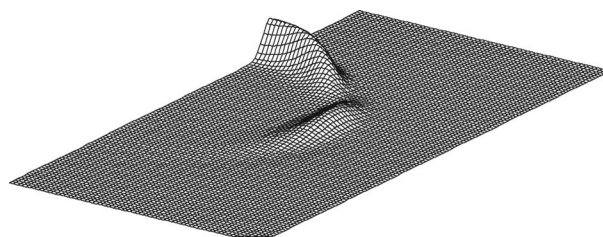

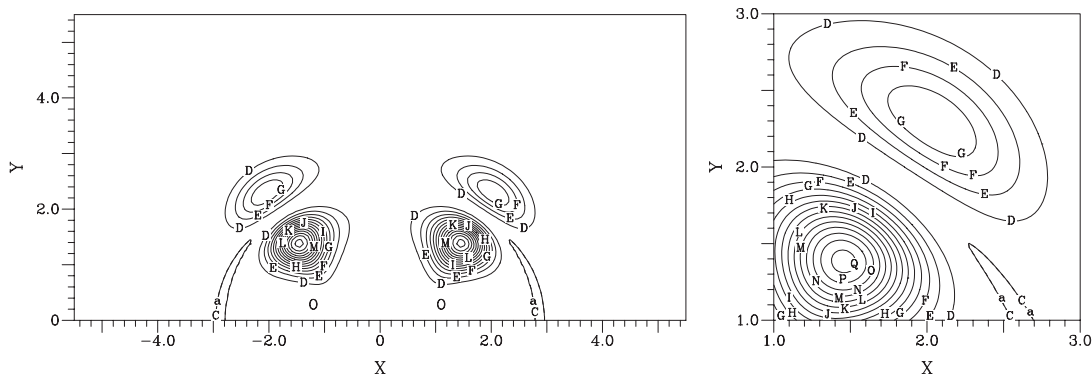FIG. 2. Perspective view for the additional term VR_{spect} for the same geometries as Fig. 1.

FIG. 3. Contour plot for the additional term VR_{spect} for a H atom moving around an equilibrium O_2 molecule with the center of the bond fixed at the origin, at the right a close view of this term near the minimum geometry. Contours are equally spaced by 0.0005 E_h, starting at -0.001 E_h.

well, for comparison we also display the original DMBE IV PES, see Fig. 4(b). We can see that both potentials have the same general features, but there are noticeable differences in the bottom well, see contours A and B.

VI. CONCLUSIONS

We have tested seven potential energy surfaces constructed for the ground state of HO_2. It would appear that none of the potentials are entirely satisfactory.

The MORBID potential of Bunker et al.[6] gives the best representation of the spectroscopic data but does not dissociate correctly. Indeed this potential does not represent the barrier between the two symmetry-related minima correctly,

a feature one would expect to influence the spectroscopy of the system at energies where tunneling splittings become significant.

The DMBE IV potential of Pastrana et al.[5] represents the global features of the HO_2 surface and gives satisfactory rotational constants. However, vibrational frequencies predicted using it are considerably in error. The discrepancies found with this potential clearly indicate the that force fields are bad input data for calibrating the potential energy surface. An attempt to rectify this problem by Varandas et al.[9] produced the DMBE IV-S potential which does indeed give good results for the known vibrational term values, but only at the expense of the rotational structure of the problem.

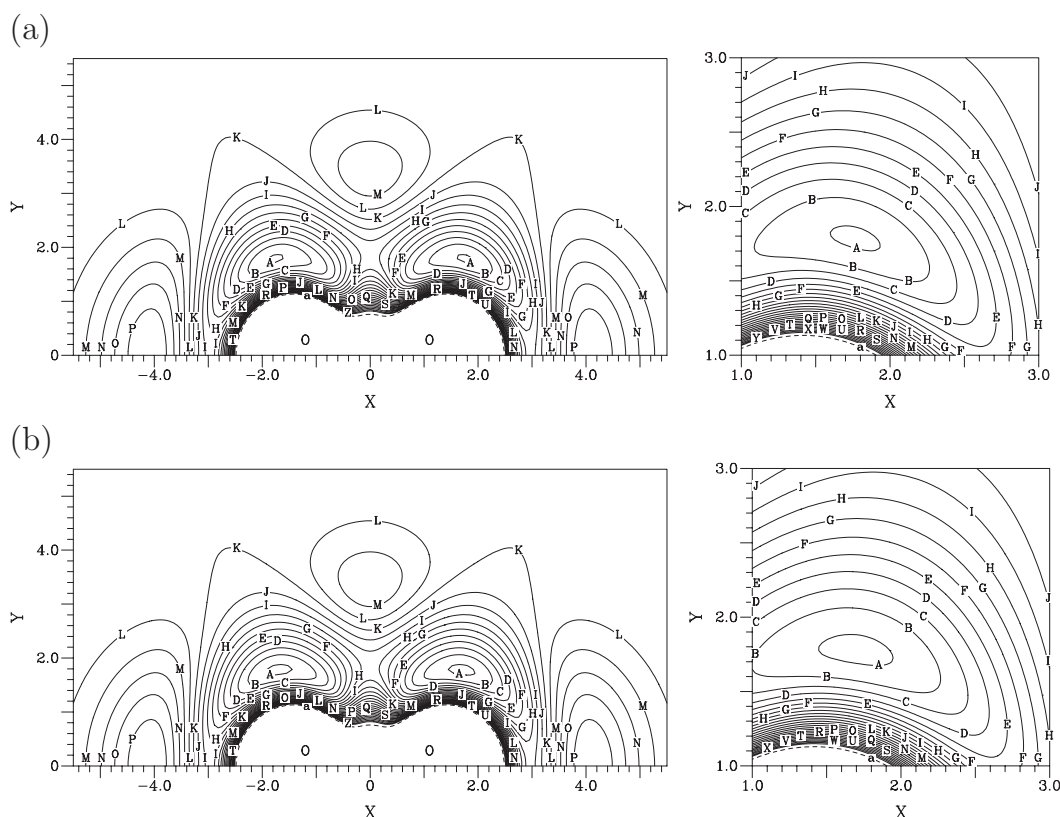The most recent potential made by Guo and co-workers

FIG. 4. Contour plot for a H atom moving around an equilibrium O_2 molecule with the bond center fixed at the origin, at the right a close view of this term near the minimum geometry. Contours are equally spaced by 0.01 E_h, starting at -0.277 E_h. (a) for the DMBE IV-VR PES and (b) for the original DMBE IV PES.

gives reasonable good results for the known vibrational term values, but the rotational structure obtained is worse than the DMBE IV and similar to the WDD and MORBID potentials.

With a small additional V_{spect} term, we have been able to correct the bottom well of the DMBE IV potential. The new DMBE IV-V PES accurately reproduces the vibrational levels giving slightly better rotational constants than those of the original DMBE IV potential. Using 13 terms in the additional VR_{spect} term, we also have been capable to fit the rotational constants. The new DMBE IV-VR PES accurately reproduces the vibrational levels (errors <0.005 cm^{-1}) and the rotational constants (root-mean-square deviation σ_{rot} $=0.0024$ cm^{-1}). While the DMBE IV-V PES conserves the equilibrium geometry and energy of the DMBE IV potential, the DMBE IV-VR potential gives small changes for this geometry and energy. Both potentials retain the remaining features of the DMBE IV PES; this is important as these play an important role in reaction dynamics on this surface for which the DMBE IV potential is known to perform well.[5]

ACKNOWLEDGMENTS

[1] M. J. Bronikowski, R. Zhang, D. J. Rakestraw, and R. N. Zare, Chem. Phys. Lett. **156**, 7 (1989).

[2] A. Viel, C. Leforestier, and W. H. Miller, J. Chem. Phys. **108**, 3489 (1998).

[3] J. Troe and V. G. Ushakov, J. Chem. Phys. **115**, 3621 (2001).

[4] S. Farantos, E. C. Leisegang, J. N. Murrell, K. Sorbie, J. J. C. Teixeira-Dias, and A. J. C. Varandas, Mol. Phys. **34**, 947 (1977).

[5] M. R. Pastrana, L. A. M. Quintales, J. Brandão, and A. J. C. Varandas, J. Phys. Chem. **94**, 8073 (1990).

[6] P. R. Bunker, I. P. Hamilton, and P. Jensen, J. Mol. Spectrosc. **155**, 44 (1992).

[7] C. E. Dateo, (unpublished), see Ref. 38.

[8] B. Kendrick and R. T. Pack, J. Chem. Phys. **102**, 1994 (1995).

[9] A. J. C. Varandas, J. M. Bowman, and B. Gazdy, Chem. Phys. Lett. **233**, 405 (1995).

[10] C. Xu, D. Xie, D. H. Zhang, S. Y. Lin, and H. Guo, J. Chem. Phys. **122**, 244305 (2005).

[11] J. N. Murrell, S. Carter, S. C. Farantos, P. Huxley, and A. J. C. Varandas, *Molecular Potential Energy Functions* (Wiley, Chichester, 1984).

[12] J. F. Ogilvie, Can. J. Spectrosc. **19**, 171 (1973).

[13] S. N. Foner and R. L. Hudson, J. Chem. Phys. **36**, 2681 (1962).

[14] A. J. C. Varandas, Mol. Phys. **53**, 1303 (1984).

[15] S. P. Walch, C. M. Rohlfing, C. F. Melius, and C. W. Bauschlicher, Jr., J. Chem. Phys. **88**, 6273 (1988).

[16] A. J. C. Varandas, J. Chem. Phys. **90**, 4379 (1989).

[17] C. F. Melius and R. J. Blint, Chem. Phys. Lett. **64**, 183 (1979).

[18] S. P. Walch and C. M. Rohlfing, J. Chem. Phys. **91**, 2373 (1989).

[19] K. G. Lubic, T. Amano, H. Uehara, K. Kawaguchi, and E. Hirota, J. Chem. Phys. **81**, 4826 (1984).

[20] H. Uehara, K. Kawaguchi, and E. Hirota, J. Chem. Phys. **83**, 5479 (1985).

[21] P. Jensen, J. Mol. Spectrosc. **128**, 478 (1988).

[22] P. Jensen, J. Chem. Soc., Faraday Trans. 2 **84**, 1315 (1988).

[23] S. P. Walch and R. J. Duchovic, J. Chem. Phys. **94**, 7068 (1991).

[24] R. P. Tuckett, P. A. Freedman, and W. J. Jones, Mol. Phys. **37**, 379 (1979).

[25] C. Yamada, Y. Endo, and E. Hirota, J. Chem. Phys. **78**, 4379 (1983).

[26] J. A. Fernley, S. Miller, and J. Tennyson, J. Mol. Spectrosc. **150**, 597 (1991).

[27] J. C. Tully, in *Semiempirical Methods of Electronic Structure Calculation*, edited by G. Segal (Plenum, New York, 1977), p. 173.

[28] P. J. Kuntz, in *Atom-Molecule Collision Theory*, edited by R. B. Bernstein (Plenum, New York, 1979), p. 79.

[29] S. P. Walch and R. J. Duchovic, J. Chem. Phys. **96**, 4050 (1992).

[30] S. P. Walch, (unpublished), see Ref. 8.

[31] A. R. W. McKellar, J. Chem. Soc., Faraday Discuss. **71**, 63 (1981).

[32] S. Y. Lin, H. Guo, P. Honvault, and D. Xie, J. Phys. Chem. B **110**, 23641 (2006).

[33] D. Xie, C. Xu, T.-S. Ho, H. Rabitz, G. Lendvay, S. Lin, and H. Guo, J. Chem. Phys. **126**, 074315 (2007).

[34] S. Y. Lin, H. Guo, P. Honvault, C. Xu, and D. Xie, J. Chem. Phys. **128**, 014303 (2008).

[35] C. Xu, B. Jiang, D. Xie, S. C. Farantos, S. Y. Lin, and H. Guo, J. Phys. Chem. A **111**, 10353 (2007).

[36] L. L. Lodi, O. L. Polyansky and J. Tennyson, Mol. Phys. **106**, 1267 (2008).

[37] C. M. A. Rio and J. Brandão, Chem. Phys. Lett. **433**, 268 (2007).

[38] V. J. Barclay, C. E. Dateo, and I. P. Hamilton, J. Chem. Phys. **101**, 6766 (1994).

[39] G. Osmann, P. R. Bunker, P. Jensen, R. J. Buenker, J.-P. Gu, and G. Hirsch, J. Mol. Spectrosc. **197**, 262 (1999).

[40] P. Jensen, G. Osmann, and P. R. Bunker, in *Computational Molecular Spectroscopy*, edited by P. Jensen and P. R. Bunker (Wiley, New York, 2000), Chap. 15, p. 485.

[41] R. P. Tuckett, P. A. Freedman, and W. J. Jones, Mol. Phys. **37**, 403 (1979).

[42] E. H. Fink and D. A. Ramsay, J. Mol. Spectrosc. **185**, 304 (1997).

[43] P. Jensen, R. J. Buenker, J.-P. Gu, G. Osmann, and P. Bunker, Can. J. Phys. **79**, 641 (2001).

[44] V. V. Melnikov, T. E. Odaka, P. Jensen, and T. Hirano, J. Chem. Phys. **128**, 114316 (2008).

[45] J. D. DeSain, A. D. Ho, and C. A. Taatjes, J. Mol. Spectrosc. **219**, 163 (2003).

[46] J. Tennyson, J. R. Henderson, and N. G. Fulton, Comput. Phys. Commun. **86**, 175 (1995).

[47] V. J. Barclay, C. E. Dateo, I. P. Hamilton, B. Kendrick, R. T. Pack, and D. W. Schwenke, J. Chem. Phys. **103**, 3864 (1995).

[48] X. T. Wu and E. F. Hayes, J. Chem. Phys. **107**, 2705 (1997).

[49] D. H. Zhang and J. Z. H. Zhang, J. Chem. Phys. **101**, 3671 (1994).

[50] V. A. Mandelshtam, T. P. Grozdanov, and H. S. Taylor, J. Chem. Phys. **103**, 10074 (1995).

[51] J. Dai and J. Z. H. Zhang, J. Chem. Phys. **104**, 3664 (1996).

[52] R. Chen and H. Guo, Chem. Phys. Lett. **277**, 191 (1997).

[53] J. M. Bowman and B. Gazdy, J. Chem. Phys. **94**, 816 (1991).

[54] B. Gazdy and J. M. Bowman, J. Chem. Phys. **95**, 6309 (1991).

[55] J. H. Schryber, O. L. Polyansky, P. Jensen, and J. Tennyson, J. Mol. Spectrosc. **185**, 234 (1997).

[56] A. Schmelzer and J. N. Murrell, Int. J. Quantum Chem. **XXVIII**, 287 (1985).

[57] R. P. Feynman, Phys. Rev. **56**, 340 (1939).

[58] D. W. Marquardt, J. Soc. Ind. Appl. Math. **11**, 431 (1963).

[59] A. Charo and F. C. de Lucia, J. Mol. Spectrosc. **94**, 426 (1982).

[60] K. Nagai, Y. Endo, and E. Hirota, J. Mol. Spectrosc. **89**, 520 (1981).

[61] J. Tennyson, *Computational Molecular Spectroscopy* (Wiley, New York, 2000), Chap. 9, p. 316.

[62] K. V. Chance, K. Park, K. M. Evenson, L. R. Zink, F. Stroh, E. H. Fink, and D. A. Ramsay, J. Mol. Spectrosc. **183**, 418 (1997).